MedChemComm

Accepted Manuscript

ROYAL SOCIETY OF CHEMISTRY

www.rsc.org/medchemcomm

Molecular dynamics and dimerization free energy analyses performed on the human Hsp90 dimer highlight dimerization hot spots and potential allosteric binding sites.

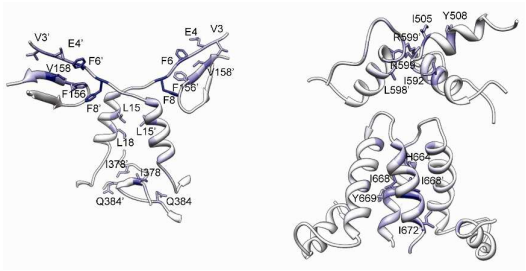

Dimerization hot spots in the structure of human Hsp90

Giulio Rastelli*

Dipartimento di Scienze della Vita, Università di Modena e Reggio Emilia. Via Campi 183, 41125 Modena (Italy)

Tel +39 059 2055145, Fax +39 059 2055131 email giulio.rastelli@unimore.it

Abstract

Dimerization is an essential step of the Hsp90 cycle. This work describes the results of a molecular dynamics and dimerization free energy analysis performed on the structure of the human Hsp90 closed dimer. Free energy decomposition on a domain- and residue- basis highlighted different dimerization hot spots within the dimer interface that could provide binding sites for the design of allosteric inhibitors.

Keywords

Hsp90, Dimerization, MM-PBSA, Molecular dynamics, Allosteric inhibitors.

Abbreviations

Heat shock protein 90 (Hsp90), N-terminal domain (NTD), middle domain (MD), C-terminal domain (CTD)

Introduction

Heat shock protein 90 (Hsp90) is an ubiquitous molecular chaperone responsible for the assembly and regulation of many signal transduction and regulatory client proteins. Since Hsp90 refolds, stabilizes and regulates the trafficking of many proteins responsible for uncontrolled proliferation and apoptotic resistance, including multiple protein kinases, steroid hormone receptors, mutated p53, survivin and others, this chaperone is an emerging target for the development of anticancer drugs.[1,2]

Hsp90 is a large and conformationally dynamic protein that undergoes dramatic conformational changes upon ATP binding and hydrolysis. Crystallography, small-angle X-ray scattering and electron microscopy techniques have revealed an underlying conformational complexity of Hsp90, which is composed by three highly dynamic domains, the N-terminal (NTD), middle (MD) and C-terminal (CTD) domains.[3] Dimerization is an essential step of the Hsp90 cycle. Recently, the crystal structure of yeast Hsp90 in complex with an ATP analogue and the co-chaperone p23/Sba1 revealed the architecture of the closed and compact homodimer, providing a view of Hsp90 in the ATP-bound state, which represents an obliged conformation along the ATPase cycle.[4]

This work reports the results of a molecular dynamics and dimerization free energy analysis performed on the structure of a human Hsp90 homology model in the closed conformation.

Decomposition of free energies on a residue basis led to the prediction of five clusters of dimerization hot spots, three of which are located in the NTD while the other two in the CTD. These residues represent valuable candidates for future mutagenesis studies and may provide new sites for the design of allosteric inhibitors.

Results and Discussion

In this investigation we have calculated free energies of dimerization of human Hsp90 in the closed conformation and then decomposed the free energy on a domain- and residue basis in order to identify possible dimerization hot spots at the dimer interface. To our knowledge, this analysis has not been performed in previous studies.

Dimerization free energies were calculated on an ensemble of structures generated with a 18 ns periodic boundary molecular dynamics simulation in water. Although such simulation time is obviously too short to sample the conformational variability along the Hsp90 cycle, it can be considered absolutely appropriate for the analysis of the free energy of dimerization of one specific conformation, i.e. that of the experimentally-validated closed, compact Hsp90 dimer. Most computational efforts were focused on the free energy analysis, which was conducted on a considerable number (nine thousand) of structural snapshots.

The averaged free energy estimates are shown in Table 1. The calculated $\Delta G'_{dimer}$ is -261±17 kcal mol^{-1}. This value should not be quantitatively compared with an experimental ΔG, because the entropic contribution $T\Delta S$ was not calculated. However, it is well recognized that entropy estimates are generally inaccurate and very time consuming, so that their inclusion may harm more than help.[5,6] Moreover, the assumption that the entropic term can be considered constant throughout the simulation is reasonable, because one specific conformation of the Hsp90 dimer was sampled. Therefore, attention should not be focused on absolute free energies but on their breakdown into domain and residue contributions.

Table 1: Domain and hot spot residue contributions to computed free energies of dimerization ($\Delta G'_{dimer}$,[(a)] kcal mol^{-1}).

Domain[(b)] contributions		Residue[(c)] contributions								
Total	-261±17	F8'	-7.1±1.0	NTD	I668	-4.1±0.7	CTD	Q384	-3.1±1.8	MD
NTD	-113±10	F8	-6.5±0.9	NTD	L18	-3.8±0.8	NTD	Y669(N)	-3.1±0.9	CTD
MD	-43±10	V158	-4.9±0.6	NTD	F156	-3.6±0.8	NTD	E4	-3.0±1.8	NTD
CTD	-105±10	F6'	-4.8±0.9	NTD	I505	-3.5±1.1	MD	L15	-2.9±0.7	NTD
		F6	-4.8±1.0	NTD	H664(F)	-3.5±0.7	CTD	I378'(L)	-2.9±0.5	MD
		V158'	-4.6±0.6	NTD	F156'	-3.4±0.8	NTD	L598'	-2.8±1.1	CTD
		I378(L)	-4.6±1.2	MD	I672'	-3.4±0.9	CTD	Y508	-2.7±0.8	MD
		I668'	-4.4±0.5	CTD	I592	-3.3±0.7	CTD	V3(S)	-2.7±0.6	NTD
		R599	-4.3±2.6	CTD	L15'	-3.3±0.6	NTD	V3'(S)	-2.7±0.4	NTD
		Q384'	-4.1±1.8	MD	E4'	-3.3±0.9	NTD	R599'	-2.7±2.1	CTD

(a) Free energies of dimerization are computed as $\Delta G'_{dimer} = \Delta E_{ELE} + \Delta E_{VdW} + \Delta G_{psolv} + \Delta G_{npsolv}$. (b) Total = NTD (N-terminal) + MD (middle) + CTD (C-terminal) domains. (c) For the sake of clarity, residues were numbered according to yeast Hsp90 (PDB code 2CG9). Prime and unprime symbols indicate residues in the two monomers. The corresponding amino acid in yeast Hsp90, when different from the one in human Hsp90, is indicated in parentheses.

Interesting conclusions can be made by analyzing separately the contribution played by the NTD, MD, and CTD (Table 1). The M domain is less involved in stabilization of the dimer, with a contribution of -43±10 kcal mol^{-1} accounting for only 16% of the total dimerization free energy. This finding is consistent with the fact that in the structure of the closed dimer the M domain is less involved in dimerization contacts and is more solvent exposed with respect to the other domains. As a matter of fact, the MD is recognized to be important for co-chaperone or client protein binding and ATP hydrolysis. On the contrary, we found that the N-terminal (-113±10 kcal mol^{-1}) and C-terminal (-105±10 kcal mol^{-1}) domains have comparable contributions, amounting respectively to 43% and 40% of the total dimerization free energy. It is well recognized that the Hsp90 dimer performs large conformational rearrangements during its functional cycle, leading to a dynamic nucleotide-dependent equilibrium between open and closed forms.[3] Our finding that both NTD and CTD are equally important for the stabilization of the dimer is in contrast with the popular view that has dominated the literature for years, according to which the CTD remains stably dimerized during the ATPase cycle, while the NTD is only transiently dimerized and is therefore solely responsible for the opening of the dimer.[7,8] However, it agrees well with more recent evidences that demonstrated, for the first time, that the CTD opens and closes with a fast kinetics and participates in the opening and closing of the dimer in concert with the NTD.[9]

To identify which residues contribute more to dimerization, the total free energy of dimerization was decomposed on a residue basis. Therefore, residues were ranked according to their contribution to $\Delta G'_{dimer}$. The results of the residue decomposition analysis revealed several groups of amino acids that contribute to the overall dimerization free energy. A graphical representation is given in Figure 1 by showing (a) the structure of the Hsp90 dimer in two different views, and (b) a color-coded representation based on residue free energy contributions, from blue to white (blue residues having the more favorable contributions). Figure 1b shows that blue residues are mainly located at the dimer interface, with a clear prevalence of residues in the NTD and CTD with respect to the MD, in agreement with the domain contributions reported in Table 1. Moreover, it clearly shows that blue residues are not equally distributed along the dimer interface but localize in well-defined regions of the structure. Therefore, hot spots of dimerization can be identified. The top thirty residues contributing to dimerization are reported in Table 1 and are graphically shown in Figure 1c and 1d. The contribution of these residues to $\Delta G'_{dimer}$ range from -7 to -2.7 kcal mol^{-1} (Table 1). Interestingly, 87% of these residues are identical between the human and yeast enzymes, and the remaining residues show conservative substitutions.

In the NTD, the first cluster of hot spot residues (V3', E4', F6', F8', V158, F156, yeast Hsp90 numbering) originates from wrapping of the N-terminal tail of one monomer to the sheet β6 of the other monomer (Figure 1c). The second cluster (V3, E4, F6, F8, V158', F156') is symmetrically placed in the other monomer (Figure 1c). The third cluster of hot spots (Figure 1c) is formed by residues of helices H1 and H1' (L15, L18, L15'), with the participation of four residues of the MD (I378, I378', Q384, Q384'). Interestingly, deletion of the first 24 amino acids in yeast Hsp90 abolished Hsp90 dimerization and ATPase activity.[10] Moreover, the L15R and L18R mutations significantly reduced ATPase activity by impairing formation of the dimer.[11] To our knowledge, besides L15 and L18, point mutations of other hot spot residues identified in this work are not available in the literature for a comparison with experimental data.

In the CTD, two clusters of hot spots were identified (Figure 1d). The first one is located in the four helix bundle formed by H20, H21 and H20', H21'(residues H664, I668, Y669, I668', I672'), and

Figure 1. (a) Structure of the full length human Hsp90 homology model in two different views. Monomers are shown in yellow and cyan. (b) Color-coded (from blue to white) representation of residue contributions to the free energy of dimerization. Residues in blue have the most favorable contributions. (c) Dimerization hot spots located in the NTD. (d) Dimerization hot spots located in the CTD.

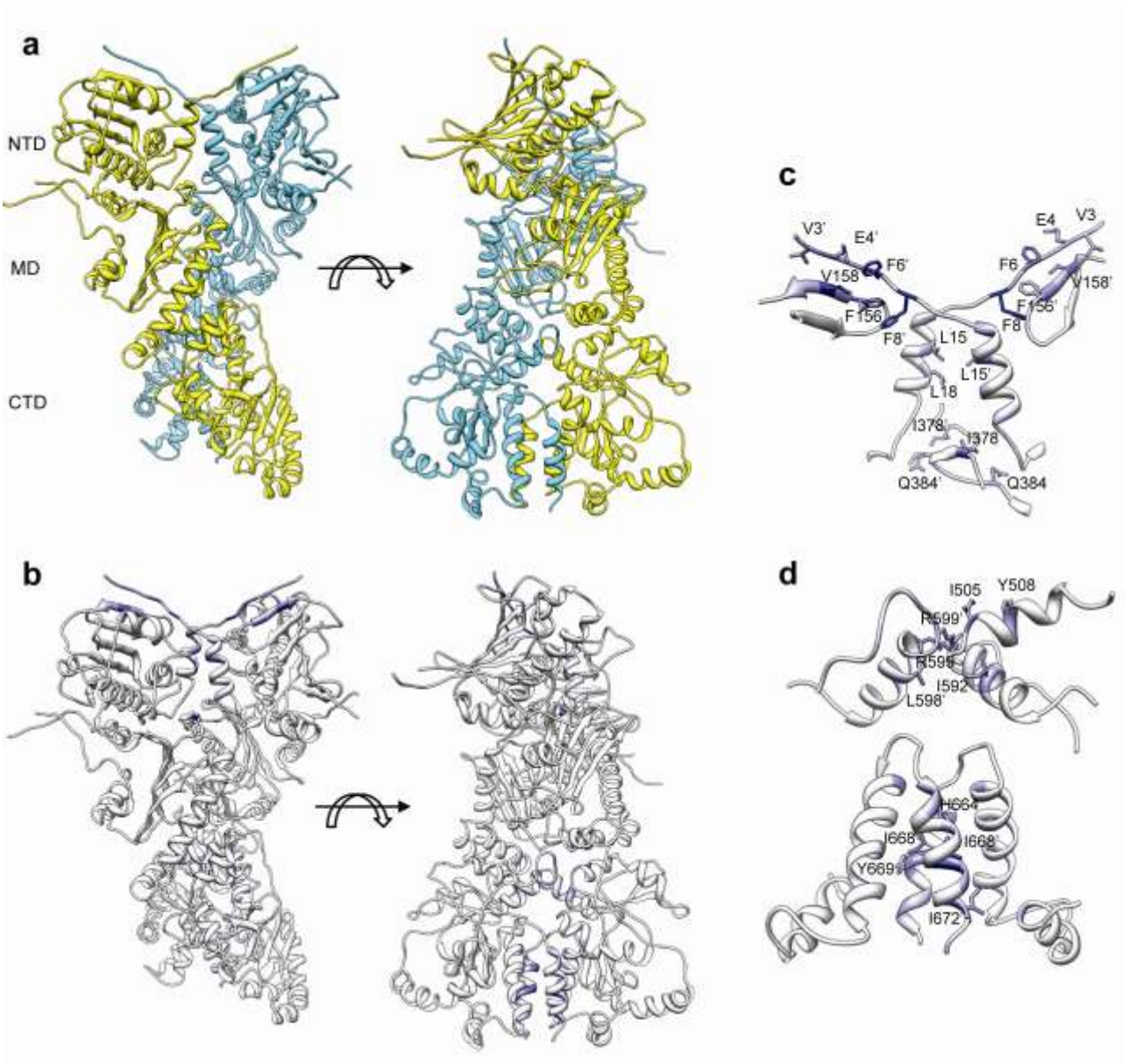

the second is between helices H18 and H18' (I592, R599, R599', L598') with the participation of two residues from the MD (I505 and Y508). It is interesting to observe that some of these CTD dimerization hot spot residues are in close proximity of a recently characterized potential allosteric pocket where the C-terminal ligand novobiocin and its coumarin derivatives were proposed to bind.[12] Moreover, the third cluster of hot spots located in the NTD (L15, L18, L15', I378, I378', Q384, Q384') encompass an additional pocket estimated as druggable by SiteMap[13] (SiteScore 1.15, Druggability Score 1.2, Exposure 0.43, Volume ~670 $Å^3$) and therefore potentially exploitable for drug design.

Conclusions

In summary, five clusters of dimerization hot spots have been identified, three of which are located in the NTD and two are in the CTD. Residues belonging to these clusters (Table 1) constitute valuable candidates for future mutagenesis studies that could validate the theoretical predictions by evaluating the impact of each residue on dimerization, which is an essential step of the Hsp90 cycle and therefore is crucial for ATPase activity. Moreover, since any small molecule able to prevent dimerization of Hsp90 would be a potential inhibitor, these hot spots may provide possible binding sites for the design of allosteric inhibitors, *i.e.* compounds that inhibit Hsp90 activity without binding to its ATP site.

Materials and Methods

Homology modeling of human full length Hsp90. An initial structure of the full length human Hsp90 dimer (chains A and B) in the closed conformation was obtained via homology modeling, using the corresponding structure of yeast Hsp90 in complex with the ATP analogue AMP-PNP[4] (PDB code 2CG9) as a template. Chain A missing residues (329-339) of 2CG9 were taken from the corresponding chain B residues. Sequences of human and yeast Hsp90 were aligned with ClustalW (63% residue identity). Homology models were built by keeping ATP in the two NTD binding sites. Moreover, four conserved and buried water molecules, which are involved in hydrogen bond networks between ATP and Asp93 or nearby residues, are not resolved in 2CG9 (resolution 3.1 Å) and were extracted from the crystal structure of Hsp90 in complex with PU3[14] (PDB code 1UY6, resolution 1.9 Å) to be included in the template for model generation with Modeller 9.[15] A thousand homology models were produced, and the best-scoring model was saved for visual inspection and further analysis. In the CTD of 2CG9, residues 598-610 (loop between helix H18 and sheet β20) are disordered. Therefore, the corresponding residues in the best-scoring homology model were subjected to loop refinement with Modeller (800 models), and the best-scoring model was saved.

Molecular dynamics simulations. Simulations were performed with the Amber 10[16] suite of programs and the ff03[17] force field.[18] The structure of the Hsp90 dimer obtained as described above was solvated in an 8 Å TIP3P octahedral box. Long-range electrostatic interactions were treated with the particle-mesh Ewald method with a grid size of 72^3 Å, a fourth-order B-spline interpolation, and a tolerance of 10^{-5}. Simulations were performed by using a residue-based cutoff of 8 Å, a time step of 2 fs and bonds involving hydrogen atoms were constrained using the SHAKE algorithm. The solvated structure was minimized with 2000 steps of conjugate gradient minimization and then gradually equilibrated at 300 K as follows: i) 20 ps of constant volume molecular dynamics with a 5 kcal mol^{-1} $Å^{-2}$ restraint on the whole protein, 600 ps of constant pressure (1atm) molecular dynamics with gradually decreasing restraints from 5 to 0 kcal mol^{-1} $Å^{-2}$, iii) 1 ns of constant pressure molecular dynamics without restraints. After equilibration, a production run of 18 ns constant pressure molecular dynamics without restraints was performed. Coordinates were collected every 2 ps, resulting in a total number of nine thousand equally spaced snapshots.

Free energy analyses. Dimerization free energies were calculated according to the equation:

$$\Delta G'_{dimer} = G_{dimer} - G_{monomer1} - G_{monomer2} \quad \text{(Eq. 1)}$$

Free energies were estimated as a sum of the following contributions:

$$G = \langle E_{int} \rangle \langle E_{ELE} \rangle + \langle E_{VdW} \rangle \langle G_{psolv} \rangle + \langle G_{npsolv} \rangle \quad \text{(Eq. 2)}$$

where E_{int}, E_{ELE}, E_{VdW} are the internal, electrostatic, and van der Waals energies calculated in the gas phase, G_{psolv} is the polar contribution to the solvation energy, and G_{npsolv} is the nonpolar solvation energy. As a single trajectory approach was adopted, differences in the internal energies canceled out and therefore did not contribute to $\Delta G'_{dimer}$.

Energies were calculated using the *mm_pbsa* module of Amber 10. The polar solvation free energies (G_{psolv}) were calculated by solving the Poisson Boltzmann (PB) equation with the Amber PBSA[19] module, with a grid spacing of 0.5Å, dielectric constants of 1 and 80 for the interior and exterior of the molecule, respectively. The dielectric boundary was defined using a 1.4 Å water probe on the atomic surface, with atomic cavity radii and atomic charges (ff03) taken from the topology files. The PB equation was solved using 1000 linear steps of finite difference.

The nonpolar solvation term (G_{npsolv}) was calculated from the solvent-accessible surface area (SASA) using the equation

$$G_{npsolv} = \gamma \, SASA + b \quad \text{(Eq. 3)}$$

where SASA was determined with the LCPO method and a probe radius of 1.4 Å. Parameters were γ=0072 kcal mol^{-1} Å^{-2} and b=0.92 kcal mol^{-1}.[5] The entropic term was not calculated.

Free energy decomposition of gas phase and PBSA desolvation energies on a per-residue basis was performed with the *mm_pbsa* module of Amber 10.[9] Visualization of structures was performed with Chimera.[20]

References

[1] J. Trepel, M. Mollapour, G. Giaccone, L. Neckers Targeting the dynamic HSP90 complex in cancer. Nature Rev. 2010, 10, 537-549.

[2] Sgobba, M., Rastelli, G. Structure-based and in silico design of Hsp90 inhibitors. ChemMedChem 2009, 4, 1399-1409.

[3] Krukenberg, K.A., Street, T.O., Lavery, L.A., Agard, D.A. Conformational dynamics of the molecular chaperone Hsp90. Quart. Rev. Biophys. 2011, 44, 229-255.

[4] Ali, M.M.U., Roe, S.M., Vaughan, C.K., Meyer, P., Panaretou, B., Piper, P.W., Prodromou, C., Pearl, L.H. Crystal structure of an Hsp90-nucleotide-p23/Sba1 closed chaperone complex. Nature 2006, 440, 1013-1017.

[5] Rastelli, G., Del Rio, A., Degliesposti, G., Sgobba, M. Fast and accurate predictions of relative binding free energies using MM-PBSA and MM-GBSA. J. Comp. Chem. 2010, 31, 797-810.

[6] Singh, N., Warshel, A. Absolute binding free energy calculations: on the accuracy of computational scoring of protein-ligand interactions. Proteins 2010, 78, 1705-1723.

[7] Wandinger, S.W., Richter, K., Buchner, J. The Hsp90 chaperone machinery. J. Biol. Chem. 2008, 283, 18473-18477.

[8] Pearl, L.H., Prodromou, C. Structure and mechanism of the Hsp90 molecular chaperone machinery. Annu. Rev. Biochem. 2006, 75, 271-294.

[9] Ratzke, C., Mickler, M., Hellenkamp, B., Buchner, J., Hugel, T. Dynamics of heat shock protein 90 C-terminal dimerization is an important part of its conformational cycle. Proc. Natl. Acad. Sci. USA. 2010, 107, 16101-16106.

[10] Richter, K., Reinstein, J., Buchner, J. N-terminal residues regulate the catalytic efficiency of the Hsp90 ATPase cycle. J. Biol. Chem. 2002, 277, 44905-44910.
[11] Vaughan, C.K., Piper, P.W., Pearl, L.H., Prodromou, C. A common conformationally coupled ATPase mechanism for yeast and human cytoplasmic HSP90s. FEBS J. 2009, 276, 199-209.
[12] Sgobba, M., Forestiero, R., Degliesposti, G., Rastelli, G. Exploring the binding site of C-terminal Hsp90 inhibitors. J. Chem. Inf. Model. 2010, 50, 1522–1528.
[13] SiteMap, version 2.5, Schrödinger, LLC, New York, NY, 2011.
[14] Wright, L., Barril, X., Dymock, B., Sheridan, L., Surgenor, A., Beswick, M., Drysdale, M., Collier, A., Massey, A., Davies, N., Fink, A., Fromont, C., Aherne, W., Boxall, K., Sharp, S., Workman, P., Hubbard, R.E. Structure-activity relationships in purine-based inhibitor binding to HSP90 isoforms. Chem. Biol. 2004, 11, 775-785.
[15] ˇSali, A., Blundell, T.L. Comparative protein modelling by satisfaction of spatial restraints. J. Mol. Biol. 1993, 234, 779–815.
[16] D.A. Case, T.A. Darden, T.E. Cheatham, III, C.L. Simmerling, J. Wang, R.E. Duke, R. Luo, M. Crowley, R.C.Walker,W. Zhang, K.M. Merz, B.Wang, S. Hayik, A. Roitberg, G. Seabra, I. Kolossváry, K.F.Wong, F. Paesani, J. Vanicek, X.Wu, S.R. Brozell, T. Steinbrecher, H. Gohlke, L. Yang, C. Tan, J. Mongan, V. Hornak, G. Cui, D.H. Mathews, M.G. Seetin, C. Sagui, V. Babin, P.A. Kollman (2008), AMBER 10, University of California, San Francisco.
[17] Duan, Y., Wu, C., Chowdhury, S., Lee, M.C., Xiong, G., Zhang, W., Yang, R., Cieplak, P., Luo, R., Lee, T., Caldwell, J., Wang, J., Kollman P.A. A point-charge force field for molecular mechanics simulations of proteins based on condensed-phase quantum mechanical calculations. J. Comput. Chem. 2003, 21, 1999-2012.
[18] Rastelli, G., Tian, Z.Q., Wang, Z., Myles, D., Liu, Y. Structure-based design of 7-carbamate analogs of geldanamycin. Bioorg. Med. Chem. Lett. 2005, 15, 5016-5021.
[19] Case, D.A., Cheatham, III T. E., Darden, T., Gohlke, H., Luo, R., Merz, Jr. K.M., Onufriev, A., Simmerling, C., Wang, B., Woods, R. The Amber biomolecular simulation programs. J. Comput. Chem. 2005, 16, 1668-1688.
[20] Pettersen, E.F., Goddard, T.D., Huang, C.C., Couch, G.S., Greenblatt, D.M., Meng, E.C., Ferrin, T.E. UCSF Chimera - A Visualization System for Exploratory Research and Analysis. J. Comput. Chem. 2004, 25, 1605-1612.